

Letter

Dynamic Event-Triggered Active Disturbance Rejection Formation Control for Constrained Underactuated AUVs

Zhiguang Feng , Senior Member, IEEE, and
Sibo Yao , Student Member, IEEE

Dear Editor,

This letter addresses the formation control problem for constrained underactuated autonomous underwater vehicles (AUVs). The feasibility condition of the virtual control law is eliminated by introducing a nonlinear state dependence function (NSDF) that transforms the state of each AUV in the formation. Then, the control scheme is constructed based on the new variables after the state transformation combined with the active disturbance rejection control (ADRC) technique to achieve asymmetric time-varying state-constrained control for each AUV. Moreover, a dynamic event-triggered mechanism (DETM) is applied to alleviate the mechanical wear of actuators, and an auxiliary dynamic system (ADS) is employed to address the input saturation. Finally, the advantages and effectiveness of the proposed method are verified by simulations.

With the development of underwater technology, the research on the control technology of multi-AUV formation has attracted much attention. Underactuated AUVs are one of the most widely applied underwater equipment, and the design of formation control schemes for them is more difficult due to their underactuated properties. Moreover, with the increasing difficulty of undersea missions, constraint control for AUVs has become a worthy research topic. Existing works usually employ the model predictive control [1], which, however, involves intricate computations. Under this background, there have been works on the problem of constrained control for the nonlinear system based on the barrier Lyapunov function [2], [3]. However, since the virtual control signal needs to be assumed to be bounded during the analysis to indirectly define the constraint bounds, it makes the results more conservative. To address this problem, NSDF based constraint control method is proposed in [4], [5], which can avoid the negative effects of feasibility conditions. However, as we observe, the problem of formation control for the constrained underactuated AUV is currently an open topic.

From a practical perspective, the complex environment and the uncertainties caused by modelling errors are also difficult for the control scheme design. As a general method to solve the lumped uncertainty, ADRC has been widely used in all kinds of unmanned system control. In addition, the actuator wear and energy consumption issues are also worth considering. In [6], a static event-triggered method is proposed, which significantly reduces times of updating the control signals. However, due to the change of system state, the static event-triggered mechanism yields more conservative results compared to the DETM [7]. Although DETM has been applied to output feedback control for marine surface vehicles [8], it is still an interesting work to apply DETM to formation control of the constrained underactuated AUV.

The main contributions in this letter are (1) A constrained underactuated AUV formation control method is proposed based on ADRC framework and a novel NSDF eliminates the virtual control law fea-

Corresponding author: Siboyao.

Citation: Z. Feng and S. Yao, "Dynamic event-triggered active disturbance rejection formation control for constrained underactuated AUVs," *IEEE/CAA J. Autom. Sinica*, vol. 12, no. 2, pp. 460–462, Feb. 2025.

The authors are with the College of Intelligent Systems Science and Engineering, Harbin Engineering University, Harbin 150001, China (e-mail: fengzhiguang@hrbeu.edu.cn; yaosibo@hrbeu.edu.cn).

Color versions of one or more of the figures in this paper are available online at <http://ieeexplore.ieee.org>.

Digital Object Identifier 10.1109/JAS.2024.124617

sibility condition. Equation (2) A DETM is introduced to reduce the number of control signal updates and thus reduce mechanical wear on the actuator. Moreover, an ADS is employed to reduce the negative influence of input saturation.

Problem statement: The dynamic model of the underactuated AUV can be expressed as follows:

$$\begin{cases} \dot{\eta}_i = R_i(\eta_i)v_i \\ M_i\dot{v}_i + C_i(v_i)v_i + D_i(v_i)v_i + g_i(\eta_i) = \tau_i + \Delta_i \end{cases} \quad (1)$$

where $\eta_i = [x_i, y_i, z_i, \theta_i, \psi_i]^T$ represents the position and orientation of the i th AUV in the earth-fixed frame, $v_i = [u_i, v_i, w_i, q_i, r_i]^T$ denotes the velocity in the body-fixed frame. $R(\eta_i)$ is the rotation matrix and $M_i = \text{diag}\{m_{11}, m_{22}, m_{33}, m_{44}, m_{55}\}$ is the inertia matrix. $C_i(v_i)$ and $D_i(v_i)$ are the Coriolis-centripetal matrix and hydrodynamic damping matrix, respectively. $g_i(\eta_i)$ denotes the restoring forces and moments. $\tau_i = [\tau_{iu}, 0, 0, \tau_{iq}, \tau_{ir}]^T$ represents the input forces and moments. Δ_i stands for the environmental disturbances. Please see [9] for more details about this dynamic model.

In practice, due to the mechanical constraints of the actuator, the control forces and moments can be described as follows:

$$\tau_{ik} = \begin{cases} \text{sign}(\tau_{ikc})\tau_{\kappa, \max}, & |\tau_{ikc}| \geq \tau_{\kappa, \max} \\ \tau_{ikc}, & |\tau_{ikc}| < \tau_{\kappa, \max} \end{cases} \quad (2)$$

where $\tau_{\kappa, \max}$ is the bound of τ_{ik} and τ_{ikc} is the command control signal.

To address the underactuated of the AUV, the following coordinate transformation is introduced:

$$\bar{\eta}_i = [x_i + \ell c(\theta_i)c(\psi_i), y_i + \ell c(\theta_i)s(\psi_i), z_i - \ell s(\theta_i)]^T \quad (3)$$

where $\ell > 0$ is the length from virtual point to the mass centre of the i th AUV. $s(\cdot)$ and $c(\cdot)$ denote sine and cosine functions, respectively.

According to (1) and (3), we can obtain

$$\begin{cases} \dot{\bar{\eta}}_i = R_{1,i}(\eta_i)\bar{v}_i + R_{2,i}(\eta_i, v_i) \\ \dot{\bar{v}}_i = F_i + \bar{M}_i^{-1}\bar{\tau}_i \end{cases} \quad (4)$$

where $\bar{v}_i = [u_i, q_i, r_i]^T$ and $\bar{\tau}_i = [\tau_{u,i}, \tau_{q,i}, \tau_{r,i}]^T$. $R_{1,i}(\eta_i)$ is the rotation matrix after the system has been transformed and $\bar{M}_i = \text{diag}(m_{11,i}, m_{44,i}, m_{55,i})$. $R_{2,i}(\eta_i, v_i)$ and F_i are nonlinear dynamics mentioned in [10].

In the sequel, we introduce assumptions as follows.

Assumption 1: The directed communication graph among the AUVs is strongly connected.

Assumption 2: The time derivative of the nonlinear function F_i is bounded, i.e., $\|\dot{F}_i\| \leq \mathcal{Y}$.

Main results: Considering the time-varying formation offsets, the state transformations are defined as $x_{i,1} = \bar{\eta}_i - \delta_i$ and $x_{i,2} = \bar{v}_i$ with δ_i is the formation offset of the i th AUV with upper bound $\bar{\delta}_i$ and lower bound $\underline{\delta}_i$. Define a compact set $\Omega_{i,h,\kappa} = \{x_{i,h,\kappa} | -\underline{x}_{i,h,\kappa}(t) < x_{i,h,\kappa}(t) < \bar{x}_{i,h,\kappa}(t)\}$, $i = 1, 2, \dots, N$, $h = 1, 2$, $\kappa = u, q, r$ with $\underline{x}_{i,h,\kappa}(t)$ and $\bar{x}_{i,h,\kappa}(t)$ are positive time-varying functions.

In order to eliminate the limitation of the feasibility condition in which virtual control laws are bounded, inspired by [5], the NSDF is constructed as follows:

$$S_{i,h,\kappa} = \frac{\bar{x}_{i,h,\kappa}\underline{x}_{i,h,\kappa}x_{i,h,\kappa}}{(\bar{x}_{i,h,\kappa} - x_{i,h,\kappa})(\underline{x}_{i,h,\kappa} + x_{i,h,\kappa})} \quad (5)$$

with the initial conditions satisfying $-\underline{x}_{i,h,\kappa}(0) < x_{i,h,\kappa}(0) < \bar{x}_{i,h,\kappa}(0)$. Differentiating $S_{i,h,\kappa}$ yields

$$\dot{S}_{i,h,\kappa} = \Gamma_{i,h,\kappa}\dot{x}_{i,h,\kappa} + \rho_{i,h,\kappa} \quad (6)$$

where $\Gamma_{i,h,\kappa} = \frac{\bar{x}_{i,h,\kappa}\underline{x}_{i,h,\kappa}(\bar{x}_{i,h,\kappa}\underline{x}_{i,h,\kappa} + x_{i,h,\kappa}^2)}{(\bar{x}_{i,h,\kappa} - x_{i,h,\kappa})^2(\underline{x}_{i,h,\kappa} + x_{i,h,\kappa})^2}$ and $\rho_{i,h,\kappa} = \frac{-\underline{x}_{i,h,\kappa}x_{i,h,\kappa}^2\dot{x}_{i,h,\kappa}}{(\bar{x}_{i,h,\kappa} - x_{i,h,\kappa})^2(\underline{x}_{i,h,\kappa} + x_{i,h,\kappa})} + \frac{\bar{x}_{i,h,\kappa}x_{i,h,\kappa}^2\dot{x}_{i,h,\kappa}}{(\bar{x}_{i,h,\kappa} - x_{i,h,\kappa})(\underline{x}_{i,h,\kappa} + x_{i,h,\kappa})^2}$.

The formation tracking control errors are defined as

$$e_{i,1} = \sum_{j=1}^M a_{ij} (S_{i,1} - S_{j,1}) + a_{i0} (S_{i,1} - S_0) \quad (7)$$

$$e_{i,2} = S_{i,2} - \alpha_i \quad (8)$$

where $S_{0,\kappa} = \frac{\bar{x}_{i,j,\kappa} \underline{x}_{i,j,\kappa} \eta_{0,\kappa}}{(\bar{x}_{i,j,\kappa} - \eta_{0,\kappa})(\underline{x}_{i,j,\kappa} + \eta_{0,\kappa})}$, and α_i being the virtual control law which will be designed later. a_{ij} and a_{i0} are the elements of the adjacency matrix between follower nodes and between leader nodes and follower nodes, respectively, as detailed in [9].

Step $i, 1$): Define $S_{i,1} = [S_{i,1,x}, S_{i,1,y}, S_{i,1,z}]^T$. Then, according to (6), we have $\dot{S}_{i,1} = \Pi_i S_{i,2} + \xi_i$, where $\Pi_i = \Gamma_{i,1} R_{1,i}(\eta_i) \beta_i$ with $\Gamma_{i,1} = \text{diag}\{\Gamma_{i,1,u}, \Gamma_{i,1,q}, \Gamma_{i,1,r}\}$, $\beta_i = (\bar{x}_{i,2,\kappa} - x_{i,2,\kappa})(\underline{x}_{i,2,\kappa} + x_{i,2,\kappa}) / (\bar{x}_{i,2,\kappa} \underline{x}_{i,2,\kappa})$ and $\xi_i = \Gamma_{i,1} R_{2,i}(\eta_i, \nu_i) - \Gamma_{i,1} \delta_i + \rho_{i,1}$.

Differentiating $e_{i,1}$ yields $\dot{e}_{i,1} = (d_i + a_{i0}) \Pi_i S_{i,2} + \zeta_{i,2}$ with $\zeta_{i,2} = -\sum_{j=1}^M a_{ij} (\Pi_j S_{j,2} + \xi_j) - a_{i0} (\Pi_0 S_{0,2} + \xi_0) + (d_i + a_{i0}) \xi_i$.

Construct the Lyapunov function as $V_{i1} = \frac{1}{2} e_{i,1}^T e_{i,1}$ for which the derivation is as follows:

$$\dot{V}_{i1} = e_{i,1}^T ((d_i + a_{i0}) \Pi_i (e_{i,2} + \alpha_i) + \zeta_{i,2}). \quad (9)$$

To simplify the structure of the virtual control law, an extended state observer (ESO) is constructed to estimate $\zeta_{i,2}$ as follows:

$$\begin{cases} \dot{\hat{\zeta}}_{i,1} = -k_{i1} [\hat{\zeta}_{i,1}]^{m_i} - k_{i2} [\hat{\zeta}_{i,1}]^{n_i} + (d_i + a_{i0}) \Pi_i S_{i,2} + \hat{\zeta}_{i,2} \\ \dot{\hat{\zeta}}_{i,2} = -k_{i3} [\hat{\zeta}_{i,1}]^{2m_i-1} - k_{i4} [\hat{\zeta}_{i,1}]^{2n_i-1} + k_{i5} \text{sign}(\hat{\zeta}_{i,1}) \end{cases} \quad (10)$$

where $\hat{\zeta}_{i,1}$ and $\hat{\zeta}_{i,2}$ are estimations of $\zeta_{i,1}$ and $\zeta_{i,2}$, respectively. $\tilde{\zeta}_{i,1} = \hat{\zeta}_{i,1} - \zeta_{i,1}$. k_{i1} , k_{i2} , k_{i3} , k_{i4} and k_{i5} are the observer gains. $m_i \in (1 - \varepsilon_i, 1)$, $n_i = 1/m_i$ with ε_i is a positive small value. $[\cdot]^g = |\cdot|^g \text{sign}(\cdot)$ with g is a positive constant and sign is the standard signum function.

Design the virtual control law α_i as follows:

$$\alpha_i = -\frac{\Pi_i^{-1}}{d_i + a_{i0}} (h_{i1} e_{i,1} + \hat{\zeta}_{i,2}) \quad (11)$$

where $h_{i2} > 0$ is control gain. Substituting (11) into (9) yields

$$\dot{V}_{i1} = -h_{i1} e_{i,1}^T e_{i,1} + e_{i,1}^T (d_i + a_{i0}) \Pi_i e_{i,2} + e_{i,1}^T \tilde{\zeta}_{i,2}. \quad (12)$$

Step $i, 2$): From (6), we have $\dot{S}_{i,2} = H_i + \Gamma_{i,2} \bar{M}_i^{-1} \bar{\tau}_i$ with $H_i = \Gamma_{i,2} F_i + \rho_{i,2}$ and $\Gamma_{i,2} = \text{diag}\{\Gamma_{i,2,u}, \Gamma_{i,2,q}, \Gamma_{i,2,r}\}$. Then, we can obtain

$$\dot{e}_{i,2} = H_i + \Gamma_{i,2} \bar{M}_i^{-1} \bar{\tau}_i - \dot{\alpha}_i. \quad (13)$$

Consider the Lyapunov function as $V_{i2} = \frac{1}{2} e_{i,1}^T e_{i,1} + \frac{1}{2} e_{i,2}^T e_{i,2} + \frac{1}{2} \varpi_i^T \varpi_i$, Differentiating V_{i2} yields

$$\begin{aligned} \dot{V}_{i2} = & e_{i,1}^T \dot{e}_{i,1} + e_{i,2}^T (H_i + \Gamma_{i,2} \bar{M}_i^{-1} \bar{\tau}_i - \dot{\alpha}_i) \\ & - (k_\varpi - 0.5) \varpi_i^T \varpi_i - \sum_{i=1}^3 |e_{i,2,\kappa} \Delta \tau_i|. \end{aligned} \quad (14)$$

Here, a tracking differentiator is established for estimating the derivative of α_i as follows:

$$\begin{cases} \dot{\varphi}_{i,1} = -\lambda_{i1} [\varphi_{i,1} - \alpha_i]^{p_{i,1}} - \lambda_{i2} [\varphi_{i,1} - \alpha_i]^{q_{i,1}} + \dot{\alpha}_i \\ \dot{\varphi}_{i,2} = -\lambda_{i3} [\varphi_{i,1} - \alpha_i]^{p_{i,2}} - \lambda_{i4} [\varphi_{i,1} - \alpha_i]^{q_{i,2}} \end{cases} \quad (15)$$

where $\varphi_{i,1}$ is the estimated value of α_i , $\varphi_{i,2}$ is an estimate for the derivative of α_i , λ_{i1} , λ_{i2} , λ_{i3} , λ_{i4} , $p_{i,1}$ and $q_{i,1}$ are positive constants, $p_{i,2} = \frac{p_{i,1}}{2-p_{i,1}}$ and $q_{i,2} = 2q_{i,1} - 1$. Owing to H_i being unknown, the ESO is constructed as follows:

$$\begin{cases} \dot{\hat{S}}_{i,2} = \hat{H}_i + \bar{\tau}_i - K_{i1} [\hat{\delta}_{i,2}]^{o_{i,1}} - K_{i2} [\hat{\delta}_{i,2}]^{o_{i,2}} \\ \dot{\hat{H}}_i = -K_{i3} [\hat{\delta}_{i,2}]^{2o_{i,1}-1} - K_{i4} [\hat{\delta}_{i,2}]^{2o_{i,2}-1} + K_{i5} \text{sign}(\hat{\delta}_{i,2}) \end{cases} \quad (16)$$

where $\hat{S}_{i,2}$ and \hat{H}_i are estimations of $S_{i,2}$ and H_i , respectively; $\hat{\delta}_{i,2}$ is the estimate error; $o_{i,1} \in (1 - \varepsilon_i, 1)$ and $o_{i,2} = 1/o_{i,1}$ with ε_i being a small constant; K_{i1} , K_{i2} , K_{i3} , K_{i4} and K_{i5} are positive constants which denote observer gains.

In order to reduce the negative influence of input saturation, set $\Delta \tau_i = \tau_i - \tau_{ic}$ and the ADS is designed as follows:

$$\dot{\varpi}_i = \begin{cases} -k_\varpi \varpi_i - \frac{\sum_{i=1}^3 |e_{i,2,\kappa} \Delta \tau_i| + 0.5 \|\Delta \tau_i\|}{\|\varpi_i\|^2} \varpi_i + \Delta \tau_i, & \|\varpi_i\| \geq \sigma \\ 0_{3 \times 1}, & \|\varpi_i\| < \sigma. \end{cases} \quad (17)$$

Then, the command control signal of the i th AUV is designed as

$$\bar{\tau}_{ic} = \bar{M}_i \Gamma_{i,2}^{-1} (-h_{i2} e_{i,2} - \hat{H}_i + \varphi_{i,2} - (d_i + a_{i0}) \Pi_i^T e_{i,1} + k_S \varpi_i). \quad (18)$$

To reduce the actuator wear, the DETM is introduced as follows:

$$\begin{aligned} \bar{\tau}_{ie,\kappa}(t) &= \bar{\tau}_{ic,\kappa}(t_k^\kappa), \quad \forall t \in [t_k^\kappa, t_{k+1}^\kappa) \quad k \in \mathbb{N} \\ t_{k+1}^\kappa &= \inf \{t \in \mathbb{R} \mid \theta_{i,\kappa} + a_\kappa (b_\kappa - |\bar{\tau}_{ie,\kappa} - \bar{\tau}_{ic,\kappa}|) \leq 0\} \end{aligned} \quad (19)$$

where a_κ and b_κ are design constants, $\theta_{i,\kappa}$ is generated by the following dynamic:

$$\dot{\theta}_{i,\kappa} = -\rho_\kappa \theta_{i,\kappa} + a_\kappa (b_\kappa - |\bar{\tau}_{ie,\kappa} - \bar{\tau}_{ic,\kappa}|). \quad (20)$$

Substituting (18) into (14) yields

$$\begin{aligned} \dot{V}_{i2} = & -h_{i1} e_{i,1}^T e_{i,1} - h_{i2} e_{i,2}^T e_{i,2} - (k_\varpi - 0.5 k_S - 0.5) \varpi_i^T \varpi_i \\ & + \Gamma_{i,2} \bar{M}_i^{-1} (\bar{\tau}_{ie} - \bar{\tau}_{ic}) + e_{i,1}^T \tilde{\zeta}_{i,2} + e_{i,2}^T \tilde{F}_i - e_{i,2}^T \tilde{\alpha}_i \end{aligned} \quad (21)$$

where $h_{i2} > 0$ is control gain. Then, combining Theorem 2 in [11] and Yang's inequality, we have

$$\begin{aligned} \dot{V}_{i2} \leq & -(h_{i1} - 0.5) e_{i,1}^T e_{i,1} - (h_{i2} - 1) e_{i,2}^T e_{i,2} \\ & - (k_\varpi - 0.5 k_S - 0.5) \varpi_i^T \varpi_i + \varsigma_i \\ \leq & -\vartheta_i V_{i2} + \varsigma_i \end{aligned} \quad (22)$$

where $\vartheta_i = \min\{2h_{i1} - 1, 2h_{i2} - 2, 2k_\varpi - k_S - 1\}$, with k_ϖ and k_S are positive constants satisfying $k_\varpi > 0.5 k_S + 0.5$. $\varsigma_i = \gamma_i + 0.5 \tilde{\zeta}_{i,2}^T \tilde{\zeta}_{i,2} + 0.5 \tilde{F}_i^T \tilde{F}_i + 0.5 \tilde{\alpha}_i^T \tilde{\alpha}_i$, with γ_i is the upper bound of $\gamma_i = \lambda_{\max}(\Gamma_{i,2} \bar{M}_i^{-1}) \|\bar{\tau}_{ie} - \bar{\tau}_{ic}\|$.

Stability analysis: To begin with, the key results of the work are summarised in the following.

Theorem 1: Consider the system containing N AUVs modeled by (1) under Assumptions 1 and 2. By employing the designed command control signal (18) and DETM (19), the multi-AUV formation tracking errors satisfy uniform ultimate boundedness and the states of the individual AUVs satisfy $-\underline{x}_{i,h,\kappa}(t) + \underline{\delta}_i < \bar{x}_{i,h,\kappa}(t) < \bar{\delta}_i$ and $x_{i,2,\kappa} \in \mathcal{Q}_{i,2,\kappa}$ i.e., $\bar{\nu}_{i,\kappa} \in \mathcal{Q}_{i,2,\kappa}$ for the initial conditions $x_{i,h,\kappa}(0) \in \mathcal{Q}_{i,h,\kappa}$.

Proof: Choose a Lyapunov function as $V = \sum_{i=1}^N V_{i2}$ for which the derivation is as follows:

$$\dot{V} = \sum_{i=1}^N (-\vartheta_i V_{i2} + \varsigma_i) \leq -\vartheta_0 V + \varsigma_0 \quad (23)$$

where $a_0 = \min\{\vartheta_i, i = 1, 2, \dots, N\}$ and $\varsigma_0 = \sum_{i=1}^N \varsigma_i$.

Combining comparison Lemma [12] and (23), we have $V(t) \leq [V(0) - \frac{\varsigma_0}{\vartheta_0}] e^{-\vartheta_0 t} + \frac{\varsigma_0}{\vartheta_0}$ which reveals that $e_{i,1}$, $e_{i,2}$ and ϖ_i are bounded. Then, by (7) combined with graph theory, we know that $S_{i,1} - S_0$ is bounded, and since S_0 is bounded, it follows that $S_{i,1}$ is bounded, which in turn ensures that $x_{i,1,\kappa} \in \mathcal{Q}_{i,1,\kappa}$. Then, we can obtain $-\underline{x}_{i,h,\kappa}(t) + \underline{\delta}_i < \bar{x}_{i,h,\kappa}(t) < \bar{\delta}_i$. Moreover, by (11) and Theorem 1 in [11], we have that $\alpha_i \in \mathcal{L}_\infty$. Since $e_{i,2}$ is bounded, we can obtain $S_{i,2}$ is bounded, which guarantees $x_{i,2,\kappa} \in \mathcal{Q}_{i,2,\kappa}$ i.e., $\bar{\nu}_{i,\kappa} \in \mathcal{Q}_{i,2,\kappa}$. ■

By Theorem 3 in [8], we can obtain that the controller designed in this work can avoid the Zeno phenomenon.

Simulation results: This section provides a simulation which justifies the validity of the proposed method. The relevant model parameters of each AUV and external environmental disturbances Δ_i are obtained from [9]. The trajectory of the virtual leader is $\eta_0 = [10 \cos(0.1t) - 10, 10 \sin(0.1t), -3 - 0.15t]$ with the asymmetric full-state constraints as $\bar{x}_{i,1,u} = 6 + 3.5 \cos(0.05t)$, $\bar{x}_{i,1,q} = 14 + 2 \sin(0.05t)$, $\bar{x}_{i,1,r} = 3 + 2 \sin(0.05t)$, $\underline{x}_{i,1,u} = 25 - 2 \sin(0.05t)$, $\underline{x}_{i,1,q} = 14 - 2 \sin(0.05t)$, $\underline{x}_{i,1,r} = 21 - 2 \sin(0.05t)$, $\bar{x}_{i,2,u} = 4 + 1 \sin(0.05t)$, $\bar{x}_{i,2,q} = 4 + 1 \sin(0.05t)$, $\bar{x}_{i,2,r} = 6 + 1 \sin(0.05t)$, $\underline{x}_{i,2,u} = 4 - 1 \sin(0.05t)$, $\underline{x}_{i,2,q} = 4 - 1 \sin(0.05t)$, $\underline{x}_{i,2,r} = 6 - 1 \sin(0.05t)$. The initial conditions for the followers can be

represented by $\eta_1(0) = [-2, -1, -4, 0, 0]$, $\eta_2(0) = [-3, -1, -5, 0, 0]$, $\eta_3(0) = [2, 1, -4, 0, 0]$ and $\eta_4(0) = [4, 1, -5, 0, 0]$. The coordinate transformation parameter $\ell = 0.2$ and the parameters of the control scheme are demonstrated in Table 1.

Table 1. Parameters of the Control Scheme

Components	Parameters
The FxESO (10)	$k_{i1} = k_{i2} = 20$, $k_{i3} = k_{i4} = 400$, $k_{i5} = 0.8$, $m_i = 2/3$, $n_i = 3/2$
The FxESO (16)	$K_{i1} = K_{i2} = 20$, $K_{i3} = K_{i4} = 400$, $K_{i5} = 0.8$, $o_{i,1} = 2/3$, $o_{i,2} = 3/2$
The FxTD (15)	$\lambda_{i1} = 1$, $\lambda_{i2} = 4$, $\lambda_{i3} = 8$, $\lambda_{i4} = 24$, $p_{i,1} = 5/7$, $q_{i,1} = 5/3$, $p_{i,2} = 5/9$, $q_{i,2} = 7/3$
The virtual control law (21)	$h_{1,i} = 5$
The command control law (18)	$h_{2,i} = 1500$, $k_{2,i} = 2.5$
The ADS (17)	$k_{\sigma} = 5$, $\sigma = 20$
The DETM (19)	$a_k = 1.0$, $b_k = 0.6$, $\rho_k = 60$

Figs. 1(a) and 1(b) display the communication topology and 3D trajectories of the AUVs, respectively. Fig. 2 shows the trajectories of individual AUVs under state constraints, which illustrates the effectiveness of the method. Fig. 3(a) shows the update of τ_{iu} , and Fig. 3(b) shows the control forces of the four AUVs with the actuator saturation boundaries set to 200, 200 and 200.

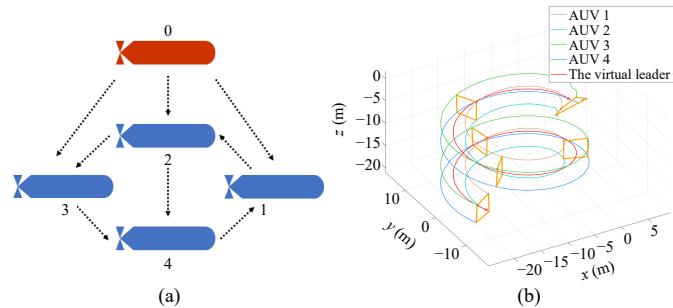


Fig. 1. Directed topology and 3D trajectories of AUVs. (a) Directed topology among four AUVs; (b) 3D trajectories of AUVs and virtual leader.

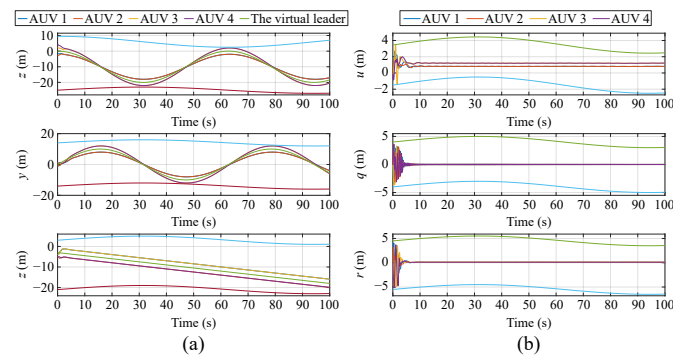


Fig. 2. Trajectories of the state for AUVs. (a) Trajectories of the position for AUVs; (b) Trajectories of the velocity for AUVs.

Conclusion: This letter has investigated the issue of the formation control for constrained underactuated AUVs. The AUV formation constraint control algorithm has been constructed based on ADRC technology and a NSDF. Then, a DETM was introduced to reduce

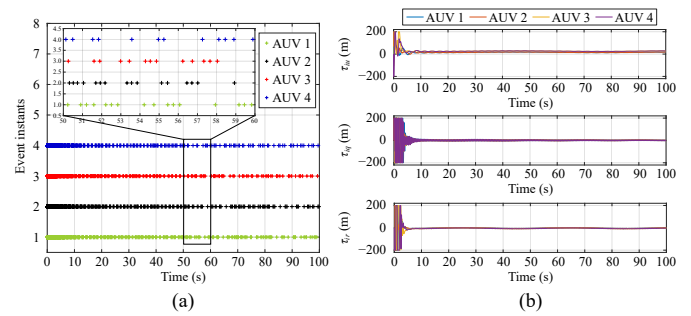


Fig. 3. Release instants and Control forces for actuators of four AUVs. (a) Release instants of four AUVs; (b) Control forces of four AUVs.

actuator wear and an ADS was used to address input saturation. Finally, a simulation has been conducted to justify the validity of the proposed method.

Acknowledgments: This work was supported by the National Natural Science Foundation of China (62073094) and the Fundamental Research Funds for the Central Universities (3072024GH0404).

References

- [1] H.L. Wei, C. Shen, and Y. Shi, "Distributed Lyapunov-based model predictive formation tracking control for autonomous underwater vehicles subject to disturbances," *IEEE Trans. Syst. Man Cybern. Syst.*, vol. 51, no. 8, pp. 5198–5208, 2021.
- [2] J. Zhang, K. Li, and Y. Li, "Output-feedback based simplified optimized backstepping control for strict-feedback systems with input and state constraints," *IEEE/CAA J. Autom. Sinica*, vol. 8, no. 6, pp. 1119–1132, 2021.
- [3] Z. Hao, X. Yue, H. Wen, and C. Liu, "Full-state-constrained non-certainty-equivalent adaptive control for satellite swarm subject to input fault," *IEEE/CAA J. Autom. Sinica*, vol. 9, no. 3, pp. 482–495, 2022.
- [4] K. Zhao and Y. Song, "Removing the feasibility conditions imposed on tracking control designs for state-constrained strict-feedback systems," *IEEE Trans. Autom. Control*, vol. 64, no. 3, pp. 1265–1272, 2019.
- [5] Z. Feng, R. Li, and L. Wu, "Adaptive decentralized control for constrained strong interconnected nonlinear systems and its application to inverted pendulum," *IEEE Trans. Neural Netw. Learn. Syst.*, vol. 35, no. 7, pp. 10110–10120, 2024.
- [6] B. Yang, Q. Zhou, L. Cao, and R. Lu, "Event-triggered control for multi-agent systems with prescribed performance and full state constraints," *Acta Autom. Sinica*, vol. 45, no. 8, pp. 1527–1535, 2019.
- [7] X. Ge, Q.-L. Han, X.-M. Zhang, and D. Ding, "Dynamic event-triggered control and estimation: A survey," *Int. J. Autom. Comput.*, vol. 18, no. 6, pp. 857–886, 2021.
- [8] G. Zhu, Y. Ma, Z. Li, R. Malekian, and M. Sotelo, "Dynamic event-triggered adaptive neural output feedback control for MSVs using composite learning," *IEEE Trans. Intell. Transp. Syst.*, vol. 24, no. 1, pp. 787–800, 2023.
- [9] J. Xu, Y. Cui, W. Xing, F. Huang, X. Du, Z. Yan, and D. Wu, "Distributed active disturbance rejection formation containment control for multiple autonomous underwater vehicles with prescribed performance," *Ocean Eng.*, vol. 259, p. 112057, 2022.
- [10] J. Du, J. Li, and F. Lewis, "Distributed 3D time-varying formation control of underactuated AUVs with communication delays based on data-driven state predictor," *IEEE Trans. Ind. Inf.*, vol. 19, no. 5, pp. 6963–6971, 2023.
- [11] K. Zhao and Y. Song, "Neuroadaptive robotic control under time-varying asymmetric motion constraints: A feasibility-condition-free approach," *IEEE Trans. Cybern.*, vol. 50, no. 1, pp. 15–24, 2020.
- [12] P. Ioannou and J. Sun, "Robust adaptive control," Upper Saddle River, USA: PTR Prentice-Hall, 1996.